NONLINEAR RESPONSE OF CONTINUOUS BRIDGE SUBJECTED TO TRAVELING SEISMIC WAVE

Kenzo Toki[I)]

SUMMARY

Dispersion curves are detected from accelerograms recorded during a past strong-motion earthquake. The phase velocity is strongly dependent on the period for the range which is important for structural response analyses. The effect of a traveling wave on a long-spanned continuous bridge is investigated considering the nonlinear behavior of the shoes. Time lag at each support exerts significant influence on the response of the axial force of the girder, the bending moment and the acceleration of the piers. The constant wave velocity assumption is sufficient for the seismic analysis for this kind of structures, which is determined from the dispersion curve as the value at the dominant frequency.

INTRODUCTION

In the usual seismic response analyses of structures, the seismic force is uniformly applied throughout the system. However, structures such as long-spanned continuous bridge and pipe lines have lengths which are of such magnitude relative to traveling seismic waves that different forces may be excited at each support. In order to clarify this effect on the structural response, the wave velocity along the ground surface must be investigated for the frequency range which is important for the structural response, accelerograms being adequate for this purpose. The first stage of this study is concerned with the detection of the wave velocity from the accelerogrsms obtained in a past strong-motion earthquake, while the traveling effects of the incident seismic wave on the structural response is discussed in the second stage.

When the ground motion model includes the Rayleigh wave component, inclination of the ground surface is induced, which forces rocking motion in the structural foundation. If the direction of wave transmission coincides with the bridge axis, the ground motion at the adjacent supports becomes out of phase and the rocking motion of the structural foundation induces higher sectional forces on the piers and girder than those due to the simultaneous excitation of each support. Thus, this study deals with the effects of the factors mentioned above on the seismic response of a long-spanned continuous bridge considering the nonlinear behavior of the shoe connections between the girder and the piers.

WAVE VELOCITY ALONG GROUND SURFACE

The accelerograms recorded at the Jet Propulsion Laboratory (JPL) and the Millikan Library (MIL) of the California Institute of Technology during the San Fernando earthquake, Feb.9, 1971, have a common time axis and thus, it is possible to detect phase velocities from them. Accelerograms at JPL

I) Professor, Disaster Prevention Res. Inst., Kyoto Univ., Kyoto, Japan.

and MIL were recorded on the basement floor of SRC and RC buildings, respectively (Hudson, Brady and Trifunac, 1971). Since the interaction between the building and soil is not significant in the building of this size during the San Fernando earthquake (Crouse and Jennings, 1973), accelerograms are considered to be close to that of the free field.

Two methods (Bloch and Hales, 1968) are employed to detect the phase velocity dispersion characteristics from these accelerograms. In the first method, the following two frequency functions are defined.

$$H_+(\omega,\tau) = \int_{-\infty}^{\infty} \{f_A(t+\tau) + f_B(t)\}\exp(-i\omega t)dt$$
$$H_-(\omega,\tau) = \int_{-\infty}^{\infty} \{f_A(t+\tau) - f_B(t)\}\exp(-i\omega t)dt \qquad (1)$$

where $f_A(t)$ and $f_B(t)$ are the seismic records at different stations A and B and τ is the time lag. Considering the function defined by

$$G(\omega,\tau) = \log_{10} \frac{H_-(\omega,\tau)}{H_+(\omega,\tau)} \qquad (2)$$

this function takes negative values when $f_A(t+\tau)$ and $f_B(t)$ is in phase and positive values when out of phase. Fig.1 illustrates the results obtained from the accelerograms in which the deepest trough marked by the dashed line represents the phase delay for each frequency component. The second method utilizes the property that a function $I(\omega_0,\tau)$ defined as the summation of the maximum value and the minimum value of a function which is a product of the out puts from a narrow band filter with the center frequency ω_0 depemds on the phase delay of the two seismic records.

Fig.2 shows the dispersion curves obtained by these two methods for the longitudinal and transverse components. It is clear from this figure that the phase velocity of the high frequency range is quite low compared with that of the low frequency component. Computing the cross spectra for two horizontal components from accelerograms at two stations, the frequency components at 1.2 Hz and 2.8 Hz are commonly observed in both spectra. Referring to Fig.2, the wave velocity at these frequencies are about 1400 m/sec and 600 m/sec respectively. Therefore, two points separated by about 700 m or 300 m between JPL and MIL would have moved in opposite directions if frequency components of 1.2 Hz or 2.8 Hz were filtered out from the ground motions. This result implies that structures which have more than one support, such as bridge or pipe line structures, are not to be treated as structures in which the seismic force is applied simultaneously to all supports.

STRUCTURAL MODEL

In order to examine the effect of the phase lag of the excitation at different supports, the bridge structure shown in Fig.3 was examined. The model is a five span continuous bridge of 600 m length, which has a hinge at the center. The piers P2 and P3 are fixed to the girder and the abutment A1 and piers P1, P2 and P4 have sliding shoes. A1, P1 and P2 are supported by soft rock and P3, P4 and P5 rest on diluvial deposits overlaying bed rock. The bridge structure is discretized into a model with 32 mass points which have three degrees of freedom (horizontal, vertical and rotation). In Fig.3, the encircled numeral expresses the mass number and the italic numeral expresses

the number of the force element which includes axial, shearing, rotation and friction springs. The springs transmitting the moment, shear and axial forces are defined in terms of the flexual stiffness, the shear modulus, the cross sectional area and the length of the element at which center the mass is attached.

Considering the deformation of adjacent elements, the following expressions are obtained under the assumption of small deformation.

$$\begin{aligned} \alpha_{i+1} &= \Phi_{i+1} - \Phi_i \\ \beta_{i+1} &= Z_{i+1} - Z_i - \frac{1}{2}(h_i\Phi_i + h_i + \Phi_{i+1}) \\ \zeta_{i+1} &= X_{i+1} - X_i \end{aligned} \tag{3}$$

The variables appearing in the above equations are defined in Figs.4 and 5.

The equation of motion of the i th mass can be written as follows:

$$\begin{aligned} m_i\ddot{X}_i &= N_{i+1} - N_i + F_{xi} \\ m_i\ddot{Z}_i &= S_{i+1} - S_i + F_{zi} \\ J_i\ddot{\Phi}_i &= M_i - M_{i+1} + h_i(S_i + S_{i+1})/2 \end{aligned} \tag{4}$$

where m_i and J_i are the mass and the mass moment of inertia of the i th mass and the other variables are defined in Fig.5. F_{xi} and F_{zi} are the reaction forces from the friction springs attached to the sliding shoe. Arranging the viscous dampers parallel to each spring, M_i, S_i and N_i are expressed as follows:

$$\begin{aligned} M_i &= k_{m,i}\,\alpha_i + C_m\dot{\alpha}_i \\ S_i &= k_{s,i}\,\beta_i + C_s\dot{\beta}_i \\ N_i &= k_{n,i}\,\zeta_i + C_n\dot{\zeta}_i \end{aligned} \tag{5}$$

where C_m, C_S and C_n are the damper coefficients and $\dot{}$ stands for the differentiation with respect to time. Substituting Eqs.(3) and (5) into Eq.(4) yields the equation of motion in terms of the displacements x and z and rotation Φ.

The foundations are assumed to be rigid and connected to the supporting ground as shown in Fig.6. The equation of motion of the foundation for horizontal displacement x_G, vertical displacement z_G and rotation angle Φ_G are obtained as follows:

$$\begin{aligned} m_G\ddot{x}_{Ga} &= -(C_H + C_s)\dot{x}_{Gr} + (SC_H + h_GC_s)\dot{\Phi}_{Gr} + C_s\dot{x}_i - \frac{1}{2}h_iC_s\dot{\Phi}_i \\ &\quad -(h_H + k_s)x_{Gr} + (Sk_H - h_Gk_s)\Phi_{Gr} + k_sx_i - \frac{1}{2}h_ik_s\Phi_i \\ m_G\ddot{z}_{Ga} &= -(C_n + C_v)\dot{z}_{Gr} + C_n\dot{z}_i - (k_n + k_v)_{Gr} + k_nz_i \\ J_G\ddot{\Phi}_{Ga} &= (SC_H - h_GC_s)\dot{x}_{Gr} - (C_n + h_G^2C_s + S^2C_H + C_R)\dot{\Phi}_{Gr} + h_GC_s\dot{x}_i \end{aligned} \tag{6}$$

$$+ (C_m - \frac{1}{2}h_G h_i C_s)\dot{\Phi}_i + (Sk_H - h_G k_s)x_{Gr} - (k_m + h_G^2 k_s + s^2 k_n + k_R)\Phi_{Gr}$$

where m_G and J_G are respectively the mass and the mass moment of inertia, and other constants are defined in Fig.6. The subscripts a and r correspond to the absolute and relative displacement. The following expressions are obtained from the variables defined above.

$$\begin{aligned} x_{Ga} &= x_{Gr} + u + b\Theta \\ z_{Ga} &= z_{Gr} + w \\ \Phi_{Ga} &= \Phi_{Gr} + \Theta \end{aligned} \tag{7}$$

in which b is the height of the center of gravity of the foundation from the bottom and u, w and Φ are the horizontal and vertical displacement and rotation of the supporting ground.

EXCITATIONS AND CASES ANALYSED

The seismic response analysis was performed in the axial direction of the bridge. The excitations are the longitudinal and vertical components of JPL and both components are applied to each foundation base considering the phase delay. The rotation angle Θ is obtained from the vertical component w of the traveling wave with the phase velocity c along the bridge axis as follows:

$$\Theta(t - \frac{x}{c}) = \frac{d}{dx}\{w(t - \frac{x}{c})\} = -\frac{1}{c}\dot{w}(t - \frac{x}{c}) \tag{8}$$

Three cases were assumed for the phase velocity: (i) the dispersion curve shown in Fig.2, (ii) constant phase velocity independent of frequency, and (iii) infinite wave velocity, meaning the simultaneous excitation of all supports.

The response analyses were performed for the ten cases listed in Table 1. In the case of the constant wave velocity, the same wave form was applied to each support considering phase delays for the wave velocity of 0.3, 0.5, 0.7, 1.0, 1.4 and 2.0 km/sec. In the case of the dispersive wave, the wave form at each support was determined from the inverse Fourier transform of the Fourier transform of the original wave, for which the phase spectrum was shifted according to the distance between the piers. Figs.7 and 8 illustrate the displacement curves at the piers P1 and P5 for the longitudinal and vertical components. Comparing the curves of Figs.7 and 8, it is obvious that the vertical component is out of phase by about $\pi/2$ to the longitudinal component, which implies that the ground motion is close to that of a Rayleigh wave.

Case 4 examine the effect of the amplification of the surficial ground on the response of the bridge. In this case, for the piers P2, P4 and P5, the excitation is applied at the rock surface and the response of the surficial ground is calculated employing the multiple reflection theory of elastic waves. The resulting wave form at the surface of the diluvial deposit is applied to the foundation base through the soil springs. For all cases except case 4, the diluvium is replaced by the base rock.

The slider shoes are on the top of piers P1, P4, P5 and abutment A1, and

are elasto-plastic as shown in Fig.9. The friction constant μ is assumed to be 0.125 or 0.5 as listed in Table 1. The foundations of piers P2 and P3 are rigid footings and that of piers P1, P4 and P5 are caissons. As this model inevitablly becomes a nonlinear system due to the elasto-plastic property of the slider and the damping property being non-proportional, the successive integration of the equation of motion (Levy and Wilkinson, 1976) was performed for a time step of 0.001 sec for the total duration of 40 seconds.

NUMERICAL RESULTS AND DISCUSSION

Figs.10 - 14 illustrate the effect of the traveling wave velocity on the sectional forces and response amplitude. The ordinate of these figures is the ratio of the response to that of the case of simultaneous excitation, while the abscissa is the wave velocity. The plots in the marginal space stands for the dispersive cases. The plots through these figures are the average of the ratios defined above for each mass and element.

Fig.10 is the result for horizontal acceleration and it is observed that the phase delay is negligible in the response acceleration of the foundation structures and the girder and that the response of the piers is magnified at least as much as about 50 percent. Fig.11 is for bending moment and this figure impies that the effect of the traveling wave on short piers is almost inversely proportional to the phase wave velocity and that, on the contrary, the bending moment is reduced when the phase lag is considered. This tendency also occurs in the case of shear force shown in Fig.12 and the effect is noticeable for relatively short piers such as P1, P4 and P5.

On the other hand, as shown in Fig.13, the phase difference exerts great influence on the axial force of the girder, especially in the case of the average ratio for the center span, which becomes more than twice the comparable value of the simultaneous excitation. Fig.14 is the result for the foundation, which indicates the effect to be negligible for the horizontal and vertical responses and shows the moderate effect on the rocking mode. The plots in the marginal space on the right hand side are close to the value for the case of 1.4 and 2.0 km/sec. The dominant frequency of the JPL record is about 0.8 - 1.5 Hz and the wave velocity at the frequency range is around 1.5 to 2.0 km/sec as seen in Fig.2. An important implication is deduced from this result, which is that the dispersion exerts negligible influence on the dynamic response of the bridge structures with the size treated herein and that the wave velocity at the dominant period range of excitation is governing the response characteristics.

Figs.15, 16 and 17 show the axial force and bending moment distribution along the girder. In these figures, the dashed line and the dotted line compare the effect of the difference of the friction coefficient and the difference between the dashed line and the solid line is due to the amplification by the surficial deposit. As the long-short line represents the distribution for the dispersive wave, it is concluded that the phase delay at the base of the foundation is most remarkable in the axial force, especially in the center span. On the contrary, the bending moment is more sensitive to differences of wave form and amplitude, which are due to the amplification of incident waves in the surficial soil layers.

CONCLUSIONS

From the analyses presented, the following can be concluded:

(1) Influence of the phase lag of the ground motion of each support is significant in the response acceleration and bending moment of piers, the axial force of the girder and the rocking motion of the foundation, while, on the contrary, the response acceleration and the bending moment of the girder is decreased compared with those of the case of simultaneous shaking.

(2) The dispersion of the traveling wave does't exert much influence on the response of the bridge and the assumption of constant wave velocity is sufficient from the engineering point of view. This wave velocity can be represented by that at the predominant period.

(3) The difference of the extent of the modification of amplitude and frequency component at each point due to the dynamic response of the surficial ground is noticeable in the bending moment of the girder and piers.

In short, when a continuous bridge is subjected to a traveling wave, while the kinetic energy is reduced owing to the fact that the piers don't move simultaneously in the same direction, the axial force is increased to resist the forces acting in the different directions through the piers. Moreover, additional shear force and bending moment are induced in the piers because of the change of the distance between the pier bottoms due to the phase difference and the rocking motion of the foundation structures, caused by the inclination of the ground.

REFERENCES

(1) Hudson, D.E., Brady, A.G. and Trifunac, M.D.: Strong-Motion Earthquake Accelerograms, Vol.II, Part G, Earthq. Eng. Res. Lab., Calif. Inst. Tech., Pasadena, 1971.

(2) Crouse, B.C. and Jennings, P.C.: Soil-Structure Interaction During the San Fernando Earthquake, Bull. Seis. Soc. Am., Vol.65, 1975, pp.13 - 36.

(3) Bloch, S. and Hales, A.L.: New Techniques for the Determination of Surface Wave Phase Velocities, Bull. Seis. Soc. Am., Vol.58, 1968, pp.921 - 1034.

(4) Levy, S. and Wilkinson, J.P.D.: The Component Element Method in Dynamics, McGraw-Hill, 1976.

(5) Toki, K.: Strain Amplitude by Body and Surface Waves in a Near Surface Ground, Proc. U.S.-Japan Seminar on Earthq. Eng. Res. with Emphasis on Lifeline Systems, 1976, pp.15 - 28.

(6) Werner, S.D.: Effects of Traveling Seismic Waves on Structure Response: A Research Program, Proc. U.S.-Japan Seminar on Earthq. Eng. Res. with Emphasis on Lifeline Systems, 1976, pp.43 - 58.

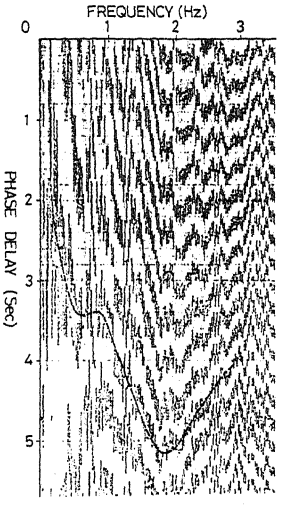

Fig.1 Phase delay time vs. frequency (TRNS comp.).

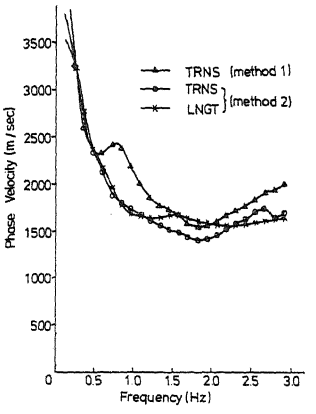

Fig.2 Dispersion curves detected by two methods.

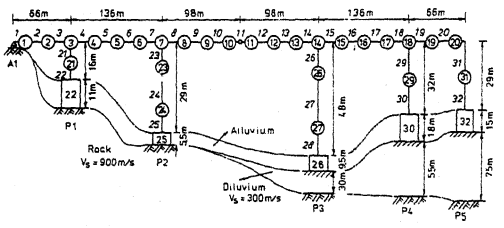

Fig.3 Analytical model.

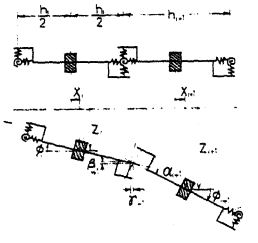

Fig.4 Beam element.

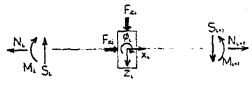

Fig.5 Coordinate system.

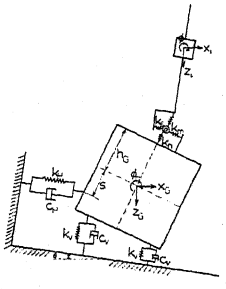

Fig.6 Analytical model of foundation.

Table 1 Cases analysed.

Case	Base Ground (P3-P5)	Phase Velocity	Soil Spring	Friction Coeff.
1	Rock	Dispersive	Standard	0.5
2	Rock	Dispersive	Standard	0.125
3	Rock	Dispersive	3S*	0.5
4	Diluvium	Dispersive	Standard	0.125
5	Rock	Constant	Standard	0.5
6	Rock	Constant	3S	0.5
7	Rock	Constant	Standard	0.125
8	Rock	Infinite	Standard	0.5
9	Rock	Infinite	Standard	0.125
10	Rock	Infinite	3S	0.5

* 3S : Three times of standard value.

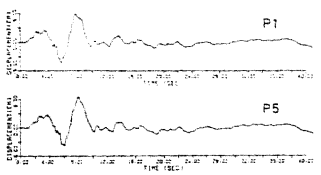

Fig.7 Displacement curves for excitation (LNGT comp.).

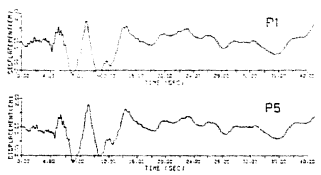

Fig.8 Displacement curves for excitation (VERT comp.).

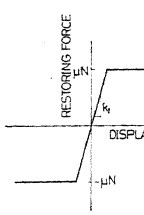

Fig.9 Restoring property of shoe.

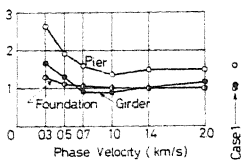

Fig.10 Effect of phase velocity on horizontal acceleration.

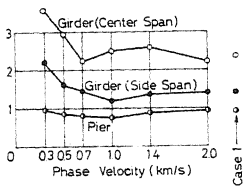

Fig.11 Effect of phase velocity on bending moment.

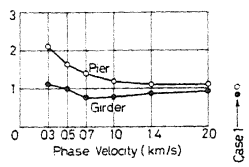

Fig.12 Effect of phase velocity on shear force.

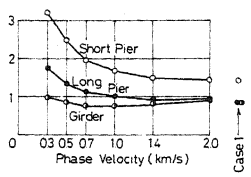

Fig.13 Effect of phase velocity on axial force.

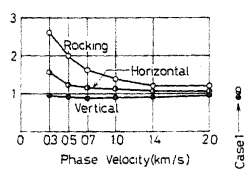

Fig.14 Effect of phase velocity on response of foundation.

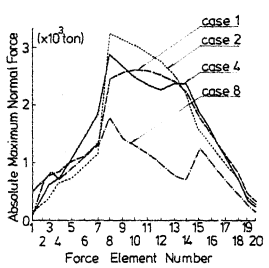

Fig.15 Distribution of maximum axial force along girder.

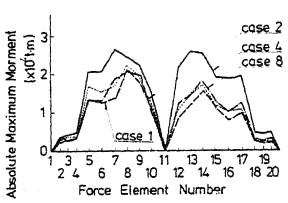

Fig.16 Distribution of maximum bending moment along girder.

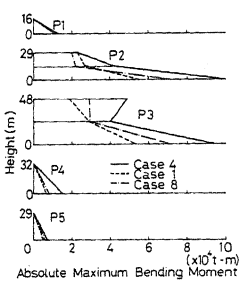

Fig.17 Distribution of maximum bending moment of piers.